BIOLOGY OF REPRODUCTION **85,** 179–188 (2011)
Published online before print 6 April 2011.
DOI 10.1095/biolreprod.110.085555

Guanine-Nucleotide Exchange Factors (RAPGEF3/RAPGEF4) Induce Sperm Membrane Depolarization and Acrosomal Exocytosis in Capacitated Stallion Sperm[1]

L.A. McPartlin,[3] P.E. Visconti,[4] and S.J. Bedford-Guaus[2,3]

Department of Clinical Sciences,[3] College of Veterinary Medicine, Cornell University, Ithaca, New York
Department of Veterinary and Animal Sciences,[4] University of Massachusetts, Amherst, Massachusetts

ABSTRACT

Capacitation encompasses the molecular changes sperm undergo to fertilize an oocyte, some of which are postulated to occur via a cAMP-PRKACA (protein kinase A)-mediated pathway. Due to the recent discovery of cAMP-activated guanine nucleotide exchange factors RAPGEF3 and RAPGEF4, we sought to investigate the separate roles of PRKACA and RAPGEF3/RAPGEF4 in modulating capacitation and acrosomal exocytosis. Indirect immunofluorescence localized RAPGEF3 to the acrosome and subacrosomal ring and RAPGEF4 to the midpiece in equine sperm. Addition of the RAPGEF3/RAPGEF4-specific cAMP analogue 8-(*p*-chlorophenylthio)-2′-*O*-methyladenosine-3′,5′-cyclic monophosphate (8pCPT) to sperm incubated under both noncapacitating and capacitating conditions had no effect on protein tyrosine phosphorylation, thus supporting a PRKACA-mediated event. Conversely, activation of RAPGEF3/RAPGEF4 with 8pCPT induced acrosomal exocytosis in capacitated equine sperm at rates (34%) similar ($P > 0.05$) to those obtained in progesterone- and calcium ionophore-treated sperm. In the mouse, capacitation-dependent hyperpolarization of the sperm plasma membrane has been shown to recruit low voltage-activated T-type Ca^{2+} channels, which later open in response to zona pellucida-induced membrane depolarization. We hypothesized that RAPGEF3 may be inducing acrosomal exocytosis via depolarization-dependent Ca^{2+} influx, as RAPGEF3/RAPGEF4 have been demonstrated to play a role in the regulation of ion channels in somatic cells. We first compared the membrane potential (E_m) of noncapacitated (−37.11 mV) and capacitated (−53.74 mV; $P = 0.002$) equine sperm. Interestingly, when sperm were incubated (6 h) under capacitating conditions in the presence of 8pCPT, E_m remained depolarized (−32.06 mV). Altogether, these experiments support the hypothesis that RAPGEF3/RAPGEF4 activation regulates acrosomal exocytosis via its modulation of E_m, a novel role for RAPGEF3/RAPGEF4 in the series of events required to achieve fertilization.

acrosome reaction, EPAC, PKA, PRKACA, RAPGEF, sperm capacitation, stallion sperm

INTRODUCTION

Ejaculated mammalian spermatozoa are not immediately able to fertilize an oocyte but acquire this ability during transit within the female reproductive tract through a process termed capacitation [1]. In several mammalian species, this process can be mimicked in the laboratory by incubating sperm in a defined medium [2–5]. Although the molecular basis of capacitation is still poorly understood, the ability of sperm to fertilize an oocyte has been correlated with time-dependent increases in protein tyrosine phosphorylation, the acquisition of acrosomal responsiveness, and the induction of hyperactivated motility in all species studied thus far (for review see [6] and [7]). Previous attempts to capacitate equine sperm in vitro have remained elusive, as evidenced by low levels of protein tyrosine phosphorylation [8, 9], low rates of acrosomal exocytosis [10–13], and low sperm-penetration rates when in vitro fertilization (IVF) has been attempted [14–20]. Recently, our laboratory has reported defined incubation conditions that yield significant time-dependent increases in protein tyrosine phosphorylation correlated with significant rates of progesterone-induced acrosomal exocytosis in equine sperm [21]. This supports the notion that protein tyrosine phosphorylation is a marker of sperm capacitation in equine sperm as it has been shown in numerous other species.

Although the molecular and biochemical changes leading to sperm capacitation are still under investigation, reports in species other than equine show that this process is associated with bicarbonate-dependent increases in intracellular cAMP levels generated by soluble adenylyl cyclase (ADCY10). Cyclic AMP then activates protein kinase A (PRKACA), a serine/threonine kinase, which then leads to downstream events including protein tyrosine phosphorylation [22]. The inhibition of ADCY10 and/or PRKACA abolishes protein tyrosine phosphorylation signaling and ultimately inhibits capacitation [23, 24]. In the horse, we demonstrated that the addition of the cAMP analog dibutyryl cAMP (dbcAMP) and phosphodiesterase inhibitor IBMX to capacitation medium increased the rate of protein tyrosine phosphorylation in stallion sperm. However, in noncapacitating medium devoid of bovine serum albumin (BSA) and/or bicarbonate, these cAMP analogues were unable to induce tyrosine phosphorylation of stallion sperm proteins [21]. This is in contrast to what has been reported in other species [2, 23], and raises the question of whether unique molecular pathways are involved in supporting capacitation-dependent events in stallion sperm.

In this regard, a family of cAMP-activated guanine-nucleotide exchange factors (RAPGEF3/RAPGEF4) has been recently discovered [25]; as a result, a comprehensive reevaluation of pathways previously attributed to cAMP-PRKACA activation is warranted. Two isoforms, RAPGEF3 and RAPGEF4, have been shown to play roles in ion channel function, intracellular calcium signaling, ion transport activity, and exocytosis in somatic cells [25]. Interestingly, RAPGEF3

[1]Supported by the Harry M. Zweig Memorial Fund for Equine Research and by start-up funds at Cornell University, College of Veterinary Medicine. Partial support was also provided by the Cooperative State Research Education Service, U.S. Department of Agriculture, Massachusetts Agricultural Experimental Station, under project MAS00907/MAS00904, and by National Institutes of Health Grants HD38082 and HD44044 (to P.E.V.).
[2]Correspondence: Sylvia J. Bedford-Guaus, Dept. of Clinical Sciences, College of Veterinary Medicine, Cornell University, T7002E VRT, Box 34, Ithaca, NY 14853. FAX 607 253 3531; e-mail: sjb55@cornell.edu

Received: 26 May 2010.
First decision: 29 June 2010.
Accepted: 17 March 2011.

eISSN: 1529-7268 http://www.biolreprod.org
ISSN: 0006-3363

has been recently identified in ejaculated human and epididymal mouse sperm [26, 27] and RAPGEF4 has been identified in mouse spermatogenic cells [28]. Given the importance of the aforementioned signal transduction pathways in sperm capacitation, it is important to revisit the regulation of these pathways, which were previously attributed to PRKACA-mediated events. Therefore, in order to investigate the roles of ADCY10, PRKACA, and RAPGEF3/RAPGEF4 in capacitation-associated events in stallion sperm, we used a variety of pharmacological agents: 1) KH7, which specifically inhibits ADCY10 and, therefore, cAMP production [24]; 2) myristolated protein kinase A inhibitor (PKI), which inhibits PRKACA activation [29]; 3) Sp-5,6-DCl-cBIMPS (cBIMPS), a cAMP analogue that is nondiscriminate in the activation of PRKACA and RAPGEF3/RAPGEF4 [30]; and 4) 8-(*p*-chlorophenylthio)-2′-*O*-methyladenosine-3′,5′-cyclic monophosphate (8pCPT), which specifically activates RAPGEF3/RAPGEF4 and not PRKACA [31]. In order to validate the use of these reagents in our laboratory, many experiments were performed side by side with both stallion and mouse sperm.

MATERIALS AND METHODS

Chemicals and Reagents

Calcium ionophore A23187 was obtained from Calbiochem (San Diego, CA). Tween 20 was purchased from BioRad (Hercules, CA). Anti-phosphotyrosine monoclonal antibody (mAB; clone 4G10; 100 μg/ml stock; raised in mouse) was purchased from Upstate Biotechnology (Lake Placid, NY). PNA-Alexa 488, valinomycin, and 3,3′-dipropylthiadicarbocyanine iodide ($DiSC_3(5)$) were purchased from Invitrogen (Carlsbad, CA). 8pCPT was purchased from BioLog Life Science Institute (San Diego, CA). PKI and cBIMPS were purchased from EMD Biosciences, Inc. (Gibbstown, NJ). The acquisition of the ADCY10 inhibitor KH7 was facilitated by Drs. Levin and Buck (Department of Pharmacology, Weill Cornell Medical College, New York, NY [24]) and purchased from the Abby and Howard P. Milistein Synthetic Chemistry Core Facility also at Weill Cornell Medical College. RAPGEF3 (N-16; 200 μg/ml; goat polyclonal IgG) and RAPGEF4 (H220; 200 μg/ml; rabbit polyclonal IgG) antibodies and RAPGEF3 peptide (N-16P; 200 μg/ml), purchased from Santa Cruz Biotechnology, Inc. (Santa Cruz, CA), were used for immunofluorescence (see Figs. 4 and 5). Donkey anti-goat fluorescein isothiocyanate (FITC)-conjugated IgG (400 μg/ml) and goat anti-rabbit FITC-conjugated IgG (400 μg/ml) were also purchased from Santa Cruz Biotechnology. The use of RAPGEF3 and RAPGEF4 antibodies purchased from FabGennix International (200 μg/ml stock, 1:100 dilution; Frisco, TX) yielded the same immunofluorescence results (see Figs. 4 and 5). For immunoblotting, however, only the latter yielded a result (see Fig. 6). In addition, for immunoblotting we also tested custom-made antibodies [27] generously donated by Dr. Claudia Tomes (Laboratorio de Biología Celular y Molecular, Instituto de Histología y Embriología–Consejo Nacional de Investigaciones Científicas y Técnicas, Facultad de Ciencias Médicas, Mendoza, Argentina), which did not cross-react with stallion sperm, and no bands were observed for RAPGEF3 or RAPGEF4. Chemicals were purchased from Sigma-Aldrich, Inc. (St. Louis, MO), unless otherwise stated.

Sperm Culture Media

Sperm were incubated as previously described [21] in modified Whittens (MW; 100 mM NaCl, 4.7 mM KCl, 1.2 mM $MgCl_2$, 5.5 mM glucose (anhydrous), 22 mM HEPES, 4.8 mM lactic acid hemicalcium salt, and 1.0 mM pyruvic acid) [32]. Negative control, noncapacitating medium was always devoid of BSA and $NaHCO_3$ and also served as transport medium. Capacitating conditions for stallion sperm were achieved by adding 25 mM $NaHCO_3$ and 7 mg/ml BSA to the noncapacitating base medium, and the final pH was adjusted to 7.25 with HCl for both conditions. Capacitating conditions for mouse sperm were achieved by adding 15 mM $NaHCO_3$ and 3 mg/ml BSA to the noncapacitating base medium, and the final pH was adjusted to 7.35 with HCl for both conditions.

Semen Collection and Preparation

The use of animals for these studies was performed in compliance with protocols approved by the Cornell University Institutional Animal Care and Use Committee. Semen was collected with an artificial vagina from seven adult stallions of proven fertility, followed by visual evaluation of sperm motility under light microscopy on a heated stage and assessment of sperm concentration using a 534B MOD1 Densimeter (Animal Reproduction Systems, Chino, CA). The sperm rich fraction, obtained by filtering the raw ejaculate through filter paper to remove the gel fraction and debris, was diluted 2:1 (vol:vol) in prewarmed noncapacitating MW and transported to the laboratory at 37°C for immediate processing. Samples were centrifuged in 15-ml conical tubes at $100 \times g$ for 1 min at 37°C to remove particulate matter and dead sperm. The supernatant was then transferred to a 14-ml round-bottom centrifuge tube and centrifuged at $600 \times g$ for 5 min at 37°C and resuspended in noncapacitating or capacitating MW to a final concentration of 10×10^6 sperm per milliliter. Samples were incubated in 500-μl aliquots in polyvinyl alcohol-coated 5-ml round-bottom tubes [33] at 37°C in a humidified air atmosphere.

Mouse epididymal sperm were isolated using a swim-out method. Briefly, epididymides were placed into 500 μl of prewarmed noncapacitating MW in a 1.5-ml round-bottom tube and allowed to swim out for 10 min in a 37°C water bath. An additional 1 ml of medium was added before centrifugation at $150 \times g$ for 5 min at room temperature. The top 1 ml of supernatant was removed, and sperm were resuspended at 6.6×10^6 sperm per milliliter. Samples were incubated in noncapacitating and capacitating MW in 300-μl aliquots in polyvinyl alcohol-coated 5-ml round-bottom tubes at 37°C.

SDS-PAGE and Immunoblotting

Stallion or mouse sperm were incubated under noncapacitating and capacitating conditions for 0, 2, 4, and 6 h or 0, 30, and 60 min, respectively, in the presence and absence of various pharmacological reagents. For RAPGEF3/RAPGEF4 immunoblotting, fresh samples were washed as above and processed immediately. Following incubation or washing, samples were then processed for SDS-PAGE and immunoblotting on 10% polyacrylamide gels as previously described [21]. Briefly, samples were washed by centrifugation, and the final pellet was resuspended in sample buffer [34] containing 40 mM dithiothreitol. Samples were then boiled for 5 min. In an attempt to isolate the full-length proteins for RAPGEF3 and RAPGEF4 (see Fig. 6), additional protein extraction methods included using a commercially available extraction buffer (Solo Buffer; Fabgennix International) as well as a RIPA buffer (10 mM Tris [pH 7.2], 150 mM NaCl, 0.1% SDS, 1% Triton X-100, 1% deoxycholate, 5 mM ethylenediaminetetraacetic acid, protease, and phosphatase inhibitors [35]).

The total volume of extract corresponding to equal numbers of sperm in each sample (5×10^6 stallion or 2×10^6 mouse sperm) was loaded on 10% SDS gels. Separated proteins were blotted onto Immobilon P membranes (Millipore, Inc., Billerica, MA) and blocked for 1 h with 1:10 (vol:vol) dilution of cold water fish skin gelatin in Tris-buffered saline + Tween 20, which was also used for all subsequent antibody incubations and washes. Immunodetection of tyrosine-phosphorylated proteins was performed using a monoclonal antibody against phosphotyrosine at a 1:10 000 dilution for 1 h and incubated for 30 min with goat anti-mouse horseradish peroxidase-coupled IgG. Immunodetection of RAPGEF3 or RAPGEF4 was performed using polyclonal antibodies at a 1:200 dilution for 3 h and incubated for 2 h with either donkey anti-goat (RAPGEF3) or goat anti-rabbit (RAPGEF4) horseradish peroxidase-coupled IgG. Immunoreactivity was visualized using enhanced chemiluminescence detection with an electrochemiluminescence kit (Amhersham Corp., Piscataway, NJ) according to the manufacturer's directions. Immunoblots shown are representative of at least three replicates with three different stallions and/or mice.

Immunofluorescence

Sperm suspensions (0.5×10^6) were washed with PBS by centrifugation ($2000 \times g$ for 2 min at room temperature), resuspended in 125 μl of PBS, and allowed to settle on glass slides for 5 min at room temperature. Excess fluid was then aspirated off, and slides were allowed to air dry. Slides were fixed in 2% paraformaldehyde for 10 min, permeabilized with 0.1% Triton X-100 in PBS, and blocked with 5% BSA in PBS for 2 h at room temperature. Primary antibodies for RAPGEF3 or RAPGEF4 (200 μg/ml stock; 1:100 in blocking solution) were added, and slides were incubated at 4°C overnight in a humidified chamber. Controls for RAPGEF3 were incubated in blocking peptide (200 μg/ml stock; 1:100 in blocking solution), and controls for RAPGEF4 were incubated in preimmune rabbit IgG (5 mg/ml in normal saline) at 4°C overnight in a humidified chamber. Slides were washed with PBS and incubated with either donkey anti-goat FITC-conjugated IgG (RAPGEF3; 400 μg/ml stock) or goat anti-rabbit FITC-conjugated IgG (RAPGEF4; 400 μg/ml stock) secondary antibodies (1:200 in blocking solution) for ≥2 h at room temperature in the dark. Slides were washed again with PBS and mounted with Vectashield (Vector Laboratories, Burlingame, CA). Slides were evaluated using an upright fluorescent Zeiss Imager ZI microscope (Thornwood, NY) with Green Fluorescent Protein (GFP) filters the following day.

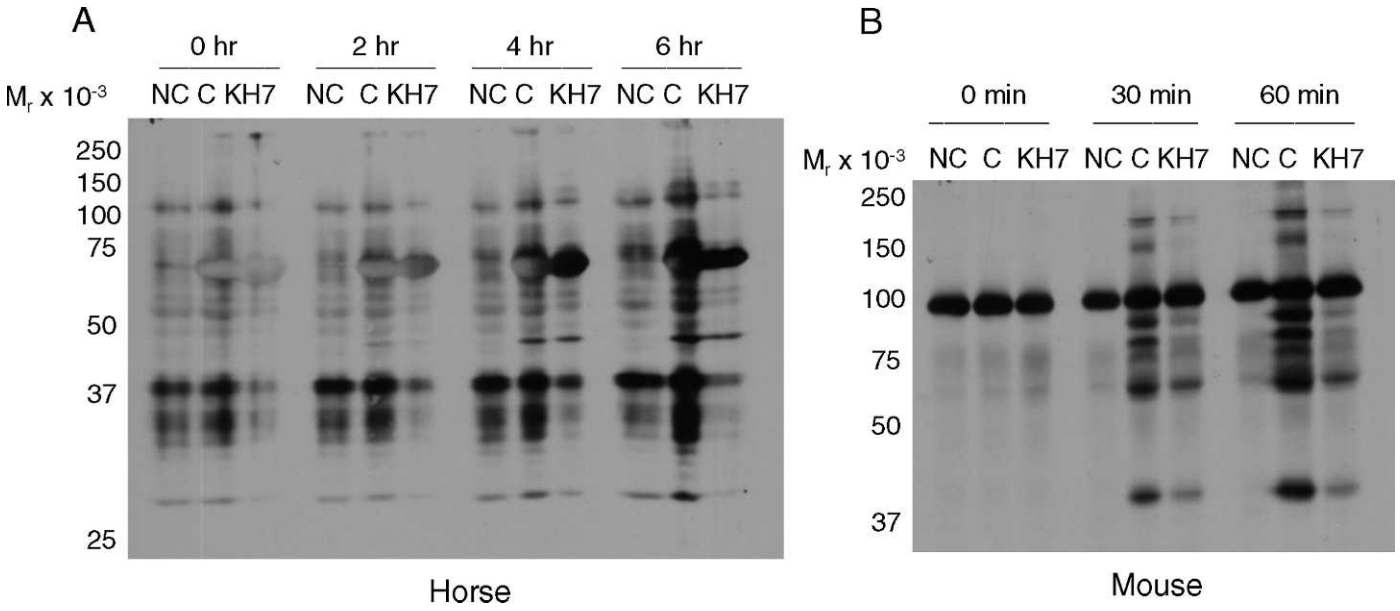

FIG. 1. Immunoblot of protein tyrosine phosphorylation in stallion (**A**) and mouse (**B**) sperm incubated in noncapacitating (NC), capacitating (C), or capacitating conditions plus the soluble adenylyl cyclase (ADCY10) inhibitor KH7. KH7 (60 μM) was used in stallion sperm incubations and 30 μM was used in mouse sperm incubations. KH7 was present in the medium from the time of collection (immediately postejaculation in the stallion or post-swim out in the mouse) and throughout the entire experiment. Experiment repeated at least three times with similar results.

Acrosome Reaction Assay

Stallion sperm were resuspended in capacitating media for 0 or 6 h. Induction of acrosomal exocytosis was performed by incubating sperm for an additional 30 min in the presence of 50 μM 8pCPT, 3 μM progesterone, 5 μM calcium ionophore A23187 [21], or an equal volume of vehicle control (dimethyl sulfoxide [DMSO]; 0.5% vol:vol). Sperm were washed with PBS by centrifugation and resuspended in 125 μl of PBS. Acrosomal status of sperm was evaluated with PNA-Alexa 488 (final concentration 0.024 mg/ml) as previously described [21]. Briefly, sperm were incubated for 10 min in the presence of PNA-Alexa 488, washed, fixed with 2% paraformaldehyde for 10 min, washed again, and mounted with Vectashield. Slides were scored (630×) for acrosomal status using the upright fluorescent Zeiss Imager ZI microscope with GFP filters. Two hundred morphologically normal sperm were counted per slide, and evaluation was performed blind of treatment status. Sperm were categorized as acrosome intact, intermediate, or acrosome reacted, as previously described [21].

Mouse sperm were incubated in capacitating medium for 0 or 1 h. Induction of acrosomal exocytosis was performed by incubating sperm for an additional 10 min in the presence of 50 μM 8pCPT, 20 μM progesterone [36], or an equal volume of vehicle control (DMSO; 0.5% vol:vol). Sperm were washed with PBS by centrifugation and fixed with 1% paraformaldehyde (400 μl total volume) for 10 min. Sperm were pelleted by centrifugation to remove fixative and washed twice with 500 μl of 100 mM sodium acetate. After the second wash, the supernatant was removed down to ~35 μl, and sperm were smeared onto slides and allowed to air dry. Slides were stained with 0.22% Coomassie blue G250 (wt:vol) in 50% methanol and 10% in acetic acid in a Coplin jar for 10 min. Slides were rinsed with PBS, air dried, and mounted with Mount-Quick (Daido Sangyo Co., Ltd., Tokyo, Japan). Acrosomal status was immediately evaluated using an Olympus BH2 microscope (100×; Center Valley, PA); staining over the acrosome indicated acrosome-intact sperm [37]. Two hundred morphologically normal sperm were counted per slide, and evaluation was performed blind of treatment status.

Membrane Potential Assay in Stallion Sperm Populations

These experiments were performed with either freshly ejaculated stallion semen or semen diluted in INRA 96 Extender (Breeder's Choice, LLC, Aubrey, TX) and cooled to 4°C during shipment in an Equitainer (Hamilton Research, Inc., South Hamilton, MA) following standard recommendations for commercial cooled shipment. Fresh semen was washed and processed as described above; cooled semen was washed from extender by dilution in room-temperature PBS and centrifugation (two to three washes at 500 × *g* for 6 min). Sperm were then resuspended at 10×10^6 sperm per milliliter (500 μl total volume) in noncapacitating, capacitating, or capacitating medium plus 50 μM 8pCPT and incubated in a 37°C water bath. Membrane potential measurements for noncapacitated sperm were taken at time points throughout the experiment, whereas sperm incubated under capacitating conditions with and without 50 μM 8pCPT were evaluated between 3 and 6 h after the initiation of incubation.

Membrane potential was measured as previously described [38]. Prior to E_m measurements, sperm were diluted in 1.5 ml total volume of either noncapacitating or capacitating medium. The fluorescent probe $DiSC_3(5)$ (1 μM final concentration) was added to the sperm suspension, followed by the addition of 1 μM carbonyl cyanide *m*-chlorophenylhydrazone (final concentration), to collapse mitochondrial membrane potential. After a 10-min incubation with these reagents (37°C), sperm suspensions were transferred to a gently stirred cuvette (37°C), and the fluorescence was continuously recorded at 620/670 nm (excitation/emission). Calibration was performed as described by Demarco et al. [38] with the addition of 1 μM valinomycin and sequential additions of KCl; membrane potential was then calculated using the Nernst equation and expressed as mV, as previously described [39].

Statistical Analysis

Raw data for percent acrosome-reacted sperm were transformed using arcsin square root and then analyzed by two-way repeated-measures ANOVA using SigmaStat software version 3.1.1 (San Jose, CA). Raw data for membrane potential was analyzed using a one-way ANOVA; when significant differences were detected ($P < 0.05$), the Student-Newman-Keuls method was applied to assess all pairwise multiple comparisons.

RESULTS

ADCY10-Generated cAMP Is Required for Capacitation-Induced Increases in Protein Tyrosine Phosphorylation in Stallion Sperm

Mammalian sperm incubated under noncapacitating conditions (i.e., without BSA and bicarbonate) do not undergo the time-dependent increases in protein tyrosine phosphorylation [5, 3, 21, 23] that are considered a hallmark of capacitation. In this regard, the ADCY10-specific inhibitor KH7 can abrogate the time-dependent increases in protein tyrosine phosphorylation in mouse sperm incubated in capacitating conditions [24]. Because capacitation-dependent protein tyrosine phosphorylation in stallion sperm requires the presence of bicarbonate in the incubation medium [21], we hypothesized that KH7 would

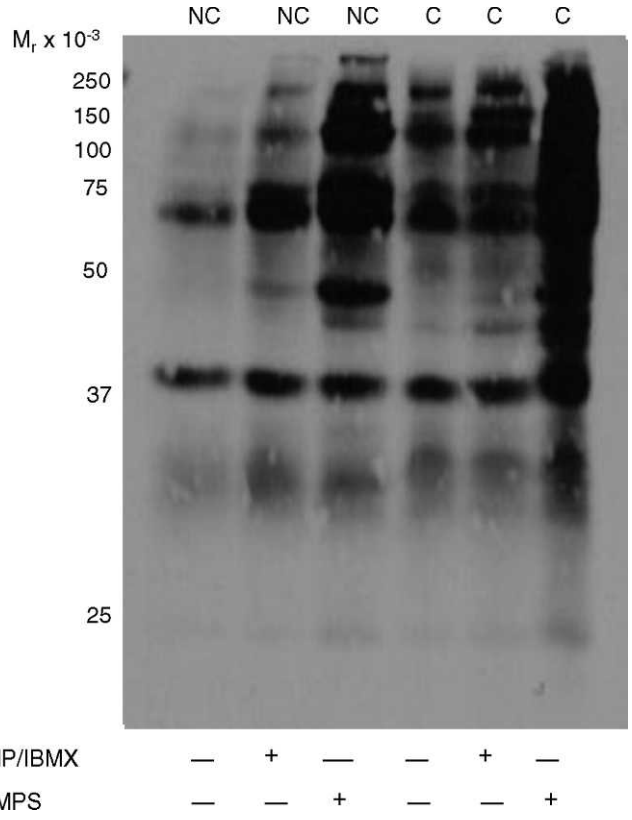

FIG. 2. Immunoblot of protein tyrosine phosphorylation in stallion sperm incubated in noncapacitating (NC), capacitating (C), or capacitating conditions in the presence of the cAMP analog cBIMPS (1 mM) or dbcAMP plus IBMX. Experiment repeated at least three times with similar results.

inhibit tyrosine phosphorylation in this species as well. We performed parallel experiments in mouse sperm as an internal laboratory control. Notably, twice the concentration of KH7 was required in stallion sperm (60 μM; Fig. 1A) to achieve the same level of inhibition obtained in mouse sperm (30 μM; Fig. 1B) [24]. Lower concentrations of KH7 (15 and 30 μM) were not sufficient to inhibit tyrosine phosphorylation in stallion sperm (data not shown). This may suggest a more robust control of these pathways in the equine sperm or perhaps inherent differences related to the origin of the sperm samples; that is, ejaculated (equine) vs. epididymal (murine) sperm, thus possibly affecting membrane permeability to KH7.

Although this experiment supports previous studies demonstrating that ADCY10 activation is responsible for protein tyrosine phosphorylation in sperm [6], we had previously reported that the combination of dbcAMP and IBMX was unable to support time-dependent increases in protein tyrosine phosphorylation in stallion sperm incubated under noncapacitating conditions (that is, in the absence of BSA and/or bicarbonate) [21]. Therefore, we tested the more membrane-permeable and phosphodiesterase-resistant cAMP analog cBIMPS. Stallion sperm incubated in noncapacitating MW plus 1 mM cBIMPS demonstrated increases in protein tyrosine phosphorylation equivalent to those observed in sperm incubated under capacitating conditions (Fig. 2). Altogether, we conclude that ADCY10-dependent cAMP production is required for the downstream capacitation-dependent protein tyrosine phosphorylation cascade in stallion sperm.

Inhibition of PRKACA Blocks the Capacitation-Dependent Increase in Protein Tyrosine Phosphorylation

Sperm capacitation research in several mammalian species points at PRKACA as being the immediate effector of ADCY10-generated cAMP leading to downstream protein tyrosine phosphorylation events [2, 6, 23]. To investigate this, we incubated stallion sperm under capacitating conditions in the presence of a sterified permeable analogue of the PRKACA-specific inhibitor PKI [32]. As shown in Figure 3A, lane 3, 60 μM PKI was required for inhibiting the capacitation-dependent increases in tyrosine phosphorylation in stallion sperm; lower concentrations of PKI (10, 20, and 30 μM) did not have the same inhibitory effect (data not shown). As a control for this pharmacological experiment, mouse sperm were also incubated under capacitating conditions in the presence of PKI. Figure 3B shows that as low as 20 μM PKI kept levels of protein tyrosine phosphorylation in mouse sperm

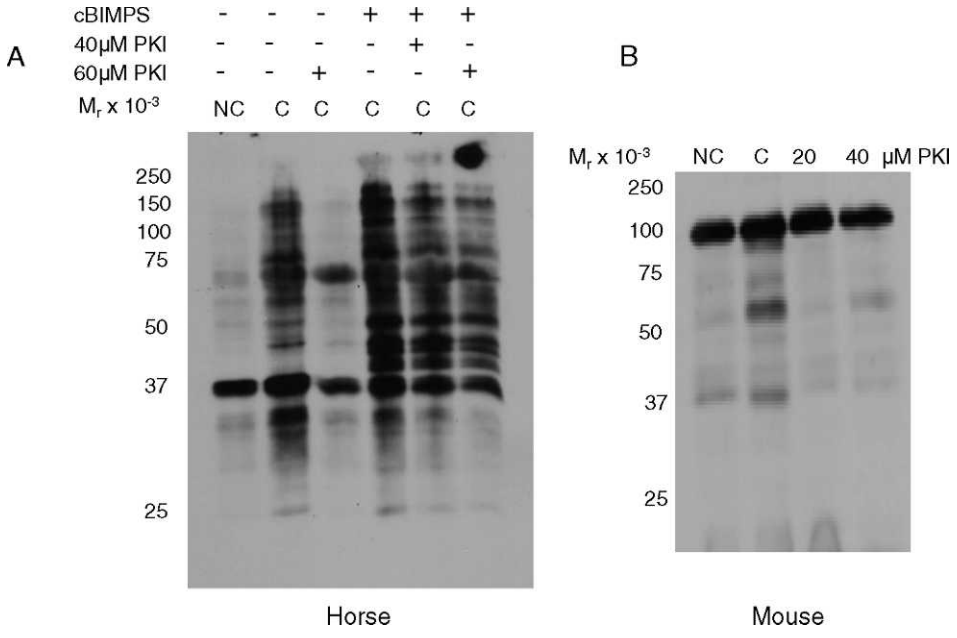

FIG. 3. Immunoblot of protein tyrosine phosphorylation in stallion (**A**) and mouse (**B**) sperm incubated in noncapacitating (NC), capacitating (C), or capacitating conditions in the presence of the cAMP analog cBIMPS (1 mM) and/or increasing concentrations of the PRKACA inhibitor PKI. PKI was present in the medium from the time of collection (immediately postejaculation in the stallion or post-swim out in the mouse) and throughout the entire experiment; cBIMPS was added at time 0 and present throughout the entire experiment. Experiment repeated at least three times with similar results.

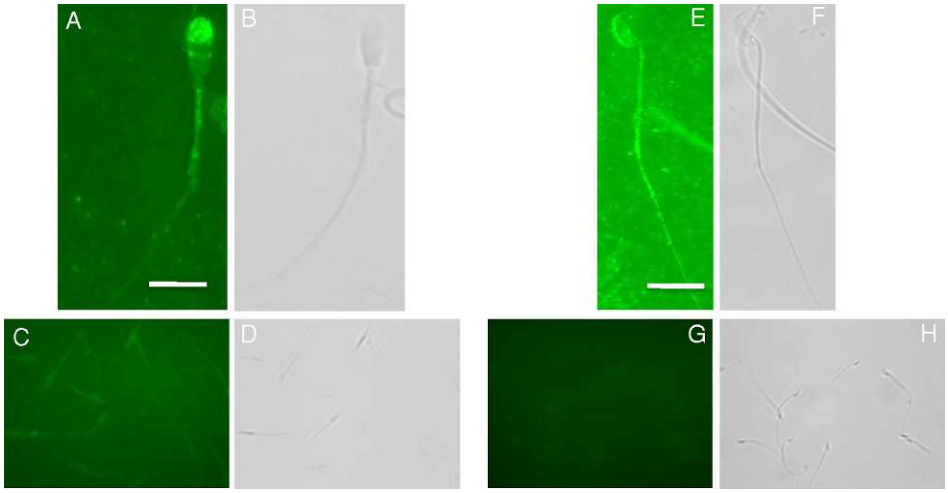

FIG. 4. Immunofluorescence localization for RAPGEF3 in stallion and mouse sperm. **A**) RAPGEF3 localizes to the acrosome and equatorial segment in stallion sperm and (**B**) corresponding bright field image. **C**) Peptide control demonstrating background levels of fluorescence and (**D**) corresponding bright field image. **E**) RAPGEF3 localizes to the acrosome in mouse sperm and (**F**) corresponding bright field image. **G**) Pre-immune rabbit IgG control demonstrating background levels of fluorescence and (**H**) corresponding bright field image. Antibodies and antigenic peptide used were purchased from Santa Cruz Biotechnology as detailed in *Materials and Methods*. Bar = 5 μm.

incubated in capacitating conditions (1 h) comparable to those observed in noncapacitated sperm.

Though these experiments supported the hypothesis that PRKACA activation is responsible for downstream protein tyrosine phosphorylation events in stallion sperm, we wanted to test the possibility that other cAMP targets contribute to these effects. For this purpose, sperm were incubated in capacitating MW with or without the PRKACA inhibitor PKI (60 μM final concentration) and the addition of 1 mM cBIMPS. The addition of cBIMPS to the capacitation medium increased the intensity of bands that showed tyrosine phosphorylation as compared to the capacitating condition alone (Fig. 3A, lane 4), as expected. Interestingly, in the presence of PKI (40 and 60 μM), sperm incubated with the addition of cBIMPS (Fig. 3A, lanes 5 and 6) still underwent tyrosine phosphorylation to levels markedly higher than those seen in the noncapacitating condition or capacitating condition with the addition of PKI alone. That is, PKI was unable to inhibit protein tyrosine phosphorylation in the presence of cBIMPS; this could suggest that the system was saturated with cAMP or, perhaps, that targets other than PRKACA may be promoting tyrosine phosphorylation events in stallion sperm.

RAPGEF3 and RAPGEF4 Are Present in Stallion and Mouse Sperm

The cAMP-dependent guanine nucleotide exchange factors RAPGEF3 and RAPGEF4 have been recently identified in somatic cells [25] and mammalian sperm [26–28]. Paired with the results above, we wanted to investigate whether RAPGEF3/RAPGEF4 may play a role downstream of cAMP in modulating protein tyrosine phosporylation events in stallion sperm.

We first investigated the expression of these proteins via indirect immuofluorescence and confirmed their presence in both stallion and mouse sperm. RAPGEF3 localized to the acrosomal membrane and/or plasma membrane overlying the acrosome and equatorial segment of stallion sperm (Fig. 4A); moreover, in agreement with previous reports, RAPGEF3 localized to the acrosomal region of mouse sperm (Fig. 4E) [26]. RAPGEF4 localized to the membrane overlying the midpiece of both stallion and mouse sperm (Fig. 5, A and E).

Immunoblotting of sperm extracts was performed using different protein extraction methods and anti-RAPGEF3 or -RAPGEF4 polyclonal antibodies from three different sources as detailed in the *Materials and Methods* section. This yielded a

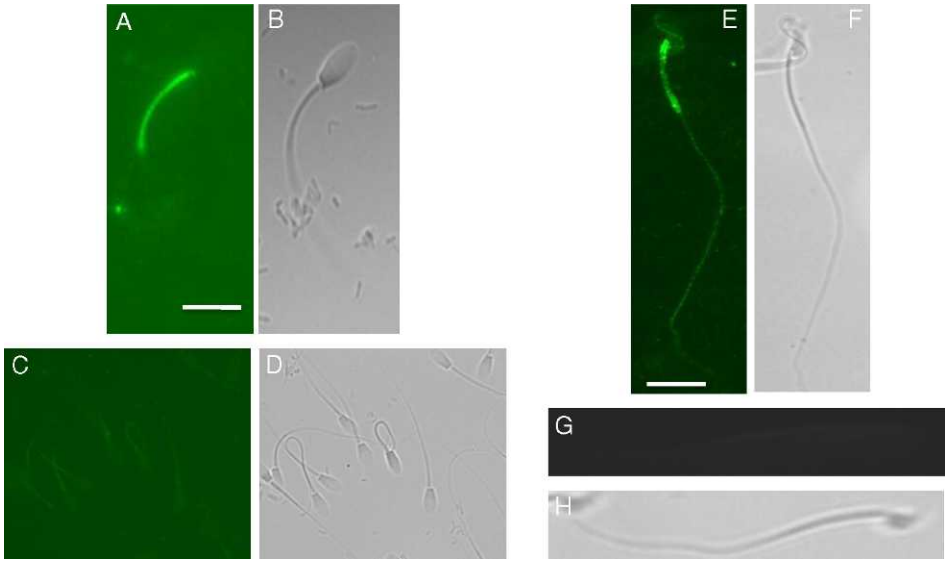

FIG. 5. Immunofluorescence localization of RAPGEF4 in stallion and mouse sperm. RAPGEF4 localizes to the midpiece in stallion (**A**) and mouse (**E**) sperm. **B** and **F**) corresponding bright field images for **A** and **E**, respectively. **C** and **G**) secondary antibody alone controls demonstrating background levels of fluorescence with corresponding (**D** and **H**) bright field images. Antibodies used were purchased from Santa Cruz Biotechnology as detailed in *Materials and Methods*. Bar = 5 μm.

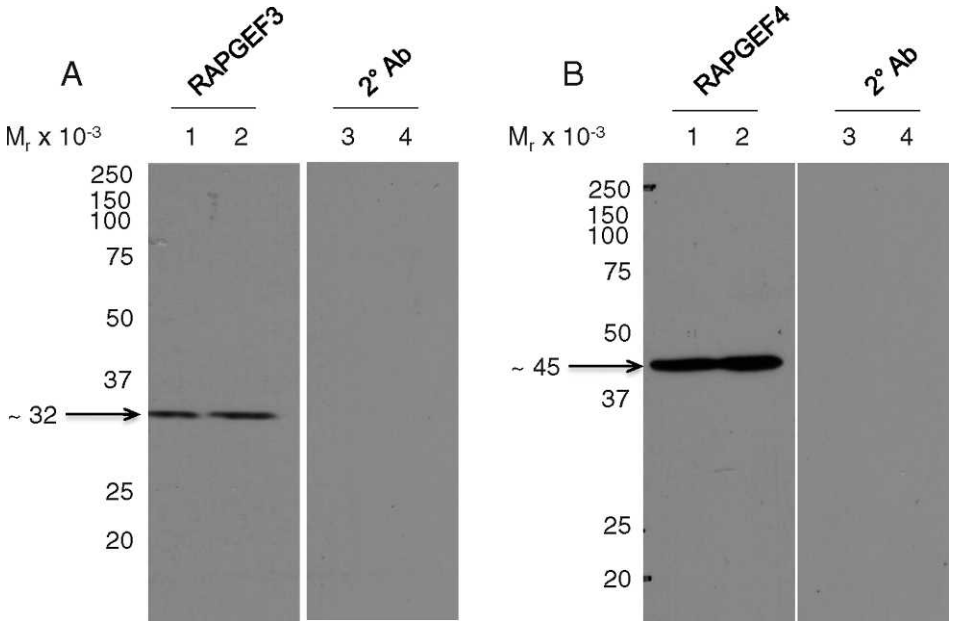

FIG. 6. Immunoblot of RAPGEF3 (**A**) and RAPGEF4 (**B**) proteins in stallion and mouse sperm. Lanes 1 and 2 are stallion and mouse sperm, respectively, incubated with primary and secondary antibodies. Lanes 3 and 4 are stallion and mouse sperm, respectively, incubated with secondary antibody alone. Antibodies used were purchased from Fab-Gennix International as detailed in *Materials and Methods*.

band at ~32 kDa (Fig. 6A; lane 1 [horse], lane 2 [mouse]) and at ~45 kDa (Fig. 6B; lane 1 [horse], lane 2 [mouse]) corresponding to RAPGEF3 and RAPGEF4 proteins, respectively. These bands did not appear when the primary antibodies were omitted (Fig. 6, A and B; lanes 3 [horse], lanes 4 [mouse]). While full-length RAPGEF3 and RAPGEF4 are 120–126 kDa in size, the observed bands correspond to the predicted sizes of the N-term regulatory subunits for these proteins, as determined by BLAST and BLAT searches of the mouse and horse genomes, respectively [25] (NCBI accession numbers NP_659099 and CAM24393; University of California, Santa Cruz horse genome browser [www.genome.ucsc.edu]). Therefore, we suspect that the protein bands observed in our immunoblotting experiments are most likely degradation products of the full-length RAPGEF3/RAPGEF4 proteins. Because there are no membrane-permeable antagonists for RAPGEF3 or RAPGEF4 available [40], we used the RAPGEF3/RAPGEF4-specific cAMP analogue 8pCPT [25] to investigate the potential involvement of these proteins in capacitation-dependent protein tyrosine phosphorylation events. For this purpose, stallion and mouse sperm were incubated under noncapacitating and capacitating conditions with and without the addition of 50 μM 8pCPT for 0, 2, and 4 h (stallion sperm) or 0, 30, and 60 min (mouse sperm). As shown in Figure 7, there was no discernable effect of 8pCPT on tyrosine phosphorylation in either incubation condition or species. These results support a primary role for a cAMP-PRKACA pathway in driving these events, as reported in other species.

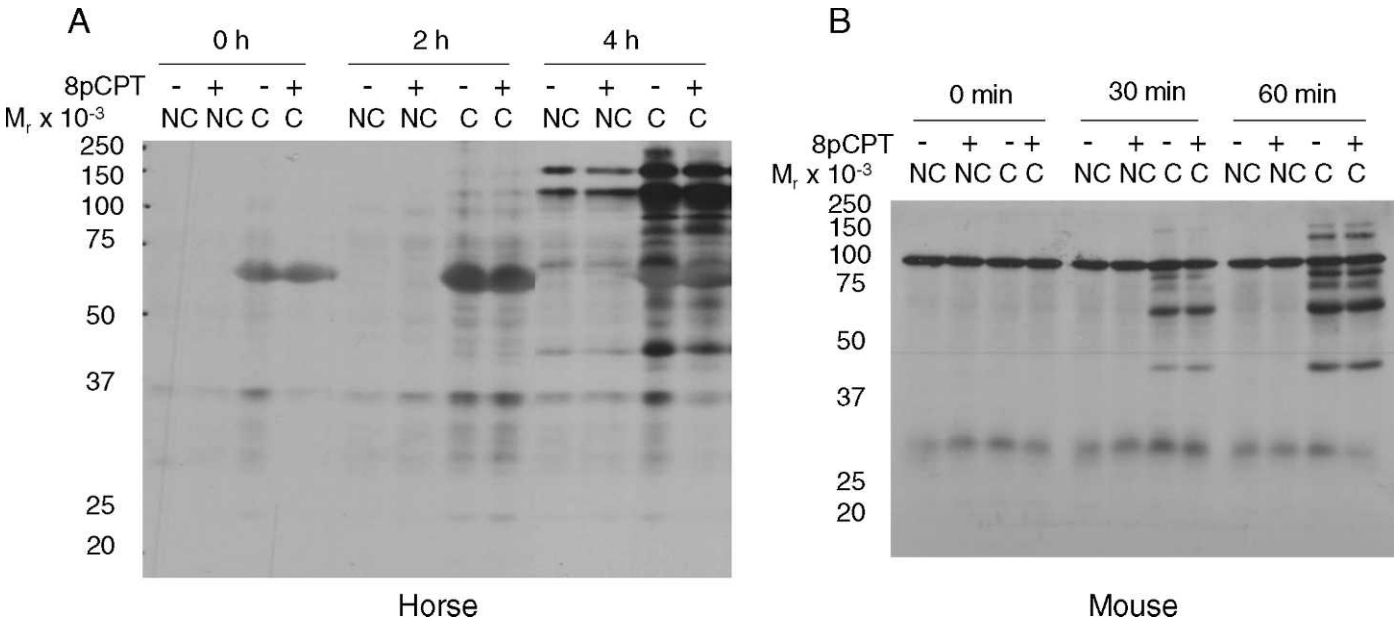

FIG. 7. Representative immunoblots of protein tyrosine phosphorylation in stallion (**A**) and mouse (**B**) sperm incubated under noncapacitating (NC) and capacitating (C) conditions in the presence (+) and absence (-) of the RAPGEF3/RAPGEF4-specific cAMP analog 8pCPT (50 μM).

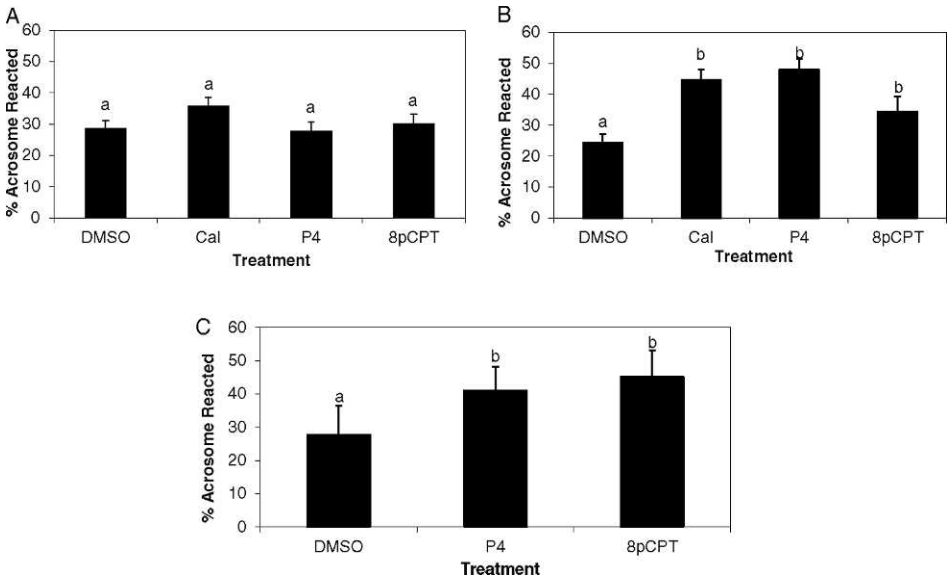

FIG. 8. Percentages of acrosomal exocytosis in stallion sperm incubated in noncapacitating (**A**) and capacitating (**B**) conditions, and of mouse sperm (**C**) incubated under capacitating conditions. After the corresponding incubations, sperm were exposed to DMSO (solvent control), calcium ionophore A23187 (Cal), progesterone (P4), or the RAPGEF3/RAPGEF4-specific cAMP analogue 8pCPT. Data are mean ± SEM; n = 3 ejaculates from 3 different stallions (**A**, **B**); n = 5 mice (**C**).

The RAPGEF3/RAPGEF4-Specific cAMP Analogue 8pCPT Induces Acrosomal Exocytosis in Capacitated Stallion and Mouse Sperm

Because RAPGEF3 localized to the acrosome (Fig. 4), we next hypothesized that its activation might play a role in the induction of acrosomal exocytosis in stallion and/or mouse sperm. In support of this, Branham et al. [27] have shown that activation of RAPGEF3/RAPGEF4 via 8pCPT in human spermatozoa contributes to the calcium-dependent phase of the acrosome reaction.

In noncapacitated (0 h) stallion sperm, 8pCPT did not induce acrosomal exocytosis, as shown in Figure 8A ($P > 0.05$). Conversely, in stallion sperm incubated under capacitating conditions (6 h), addition of 8pCPT (presumably activating RAPGEF3) induced 34.3% acrosomal exocytosis rates, which was higher ($P = 0.03$) than those obtained in DMSO-vehicle treated controls (24.2%; Fig. 8B). Moreover, this percentage was similar ($P > 0.05$) to rates achieved with both progesterone and calcium ionophore (47.9% and 44.5%, respectively; Fig. 8B). Similarly, in mouse sperm, 8pCPT induced 45% exocytosis rates (Fig. 8C), which were higher ($P = 0.004$) than DMSO-treated controls (27.5%) but comparable ($P > 0.05$) to rates achieved with progesterone (47.9% acrosomal exocytosis). From these studies, we concluded that activation of RAPGEF3 via 8pCPT induces acrosomal exocytosis in capacitated stallion and mouse sperm.

8pCPT Maintains Sperm Plasma Membrane in the Depolarized State

Hyperpolarization of the sperm plasma membrane, which has been demonstrated to occur during capacitation, is required for fertility [38, 39, 41]. Currently, cAMP is believed to play a role in hyperpolarization of the sperm plasma membrane through a PRKACA-mediated pathway [42]; however, in various somatic cell lines, activation of RAPGEF3/RAPGEF4 via 8pCPT has been shown to have effects on ion channels known to play a role in the modulation of E_m [31, 43–45]. The potential role of RAPGEF3/RAPGEF4 in this event has not been investigated in mammalian sperm. For this purpose, stallion sperm were incubated in noncapacitating, capacitating, and capacitating medium with the addition of 50 μM 8pCPT for up to 6 h. Figure 9 shows representative E_m tracings for noncapacitated sperm (Fig. 9A) and capacitated sperm incubated in the absence (Fig. 9B) and presence of 8pCPT (Fig. 9C). Membrane potential of noncapacitated sperm was measured throughout the experiment; E_m for sperm incubated under capacitating conditions with and without 8pCPT was measured between 3–6 h after the initiation of incubation. Equine sperm die quickly after undergoing acrosomal exocytosis; therefore, sperm motility was monitored for all conditions prior to recording. Noncapacitated stallion sperm displayed a resting mean E_m of −37.11 mV vs. capacitated sperm, which hyperpolarized to −53.74 mV ($P = 0.002$). Interestingly, when sperm were incubated under capacitating conditions in the presence of 8pCPT, sperm E_m was maintained in the depolarized state at −32.06 mV; this result was comparable ($P > 0.05$) to noncapacitated sperm but different ($P < 0.001$) from capacitated sperm (Fig. 9D). Therefore, this experiment not only determined the resting and capacitation-associated E_m for stallion sperm, but also demonstrates that RAPGEF3 and/or RAPGEF4 activation play a role in maintaining the sperm plasma membrane in a depolarized state.

DISCUSSION

Our previous work suggested inherent differences in the physiological response of stallion sperm to pharmacological agents used to ascertain the pathways linked to sperm capacitation [21]. Moreover, the recent discovery of cAMP-dependent guanine nucleotide exchange factors RAPGEF3 and RAPGEF4 in somatic and germ cells prompted the reevaluation of pathways previously attributed to cAMP-PRKACA activation. Therefore, in this study, we sought to separate the roles of PRKACA and RAPGEF3/RAPGEF4 in the events required to achieve fertilization competency in stallion sperm.

Though it is widely reported that capacitation-dependent protein tyrosine phosphorylation follows a cAMP-PRKACA-driven pathway [6], we have previously shown that the addition of dbcAMP-IBMX to noncapacitating medium was unable to support time-dependent increases in protein tyrosine phosphorylation in stallion sperm [21], contrary to what has been shown in all other species studied. This prompted us to further investigate these pathways in stallion sperm. In this study we show that a specific inhibitor of ADCY10, KH7, is able to reduce protein tyrosine phosphorylation to levels similar to those observed in the noncapacitating condition. Notably, the

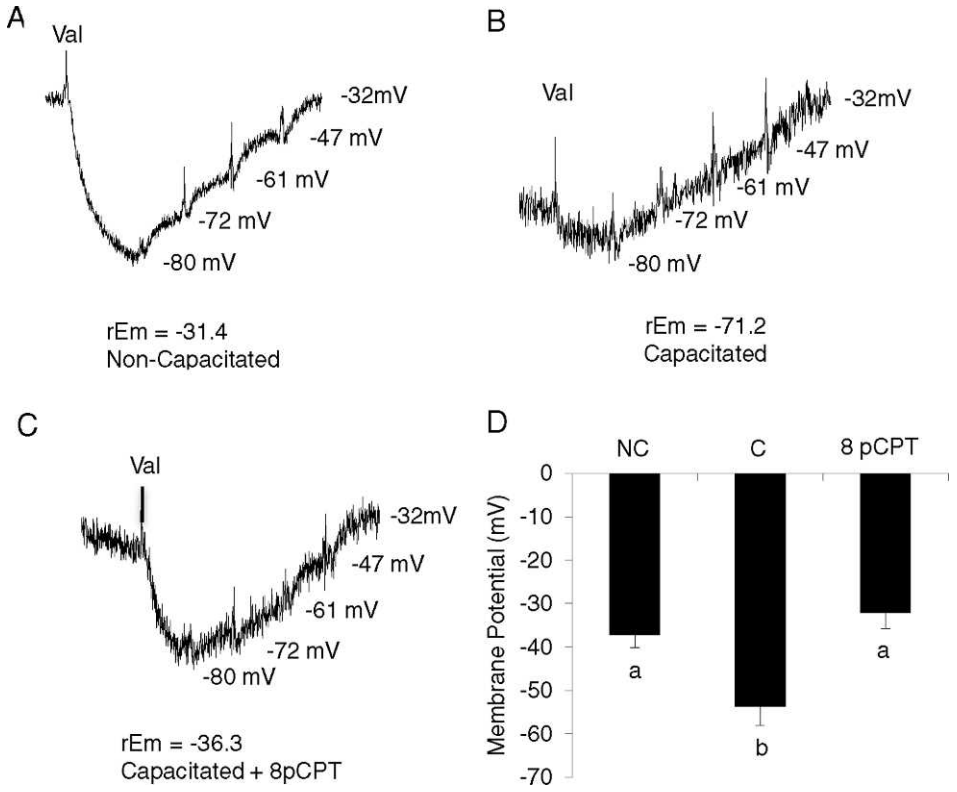

FIG. 9. Representative membrane potential (E_m) tracings of noncapacitated stallion sperm (**A**), capacitated stallion sperm (**B**), and sperm incubated under capacitating conditions in the presence of 8pCPT (**C**). **D**) Average E_m of noncapacitated stallion sperm (NC), capacitated stallion sperm (C), and stallion sperm incubated under capacitating conditions in the presence of 8pCPT (8P) Data are mean ± SEM; n = 3 ejaculates from three different stallions.

higher concentrations of KH7 required to inhibit protein tyrosine phosphorylation in stallion vs. mouse sperm may reflect a more robust control of these pathways and/or may be a consequence of sperm origin, i.e., ejaculated (stallion) vs. epididymal (mouse). Ejaculated stallion sperm are exposed to bicarbonate in seminal plasma and, thus, this may also explain that some levels of protein tyrosine phosphorylation are observed already at time 0 or in samples incubated in noncapacitating conditions, albeit relatively lower than those in the capacitating condition.

Additionally, we suspected that a highly active phosphodiesterase not inhibited by IBMX may have been responsible for the lack of effect observed when incubating stallion sperm in the presence of dbcAMP-IBMX [21]. In support of this assumption, in this study cBIMPS, a nondegradable cAMP analogue, was able to support increases in tyrosine phosphorylation levels in sperm incubated in the absence of BSA and/or bicarbonate. However, because cBIMPS is a nonspecific cAMP analogue, we next tested the role of PRKACA in this pathway. Previous reports show that PKI can inhibit protein tyrosine phosphorylation in mouse sperm; however, in our study PKI was unable to completely abolish time-dependent increases in protein tyrosine phosphorylation in stallion sperm incubated under capacitating conditions, and in particular when cBIMPS was also added to the incubation medium.

The above findings and the recent discovery of RAPGEF3/RAPGEF4 as downstream effectors of cAMP prompted us to hypothesize that these proteins might play a role in capacitation-associated protein tyrosine phosphorylation in stallion sperm. In one-dimensional gel electrophoresis, however, we were unable to detect any changes in phosphotyrosine levels when the RAPGEF3/RAPGEF4-specific activator 8pCPT was added to the incubation medium in both stallion or mouse sperm. Under capacitating conditions, any additional effects of 8pCPT may have been masked by the already marked levels of protein tyrosine phosphorylation typical of sperm incubated in this condition. Under noncapacitating conditions, the absence of BSA and/or bicarbonate may have precluded appropriate membrane permeability of the cAMP analogue (particularly in stallion sperm, which are ejaculated and, therefore, coated by seminal plasma components). To be certain that our negative results were not due to membrane permeability issues, we incubated stallion sperm under noncapacitating conditions plus 8pCPT in the presence of BSA. Again, we observed no effect of RAPGEF3/RAPGEF4 activation on tyrosine phosphorylation, and levels remained comparable to the noncapacitating condition (data not shown). Moreover, we reasoned that the observation that PKI does not completely inhibit tyrosine phosphorylation in the presence of cBIMPS might have been likely due to the saturation of cAMP out-competing the inhibition of PRKACA. Altogether, these results suggest that RAPGEF3/RAPGEF4 are not involved in the cAMP-induced increase in tyrosine phosphorylation and support the notion that protein tyrosine phosphorylation follows a cAMP-PRKACA-driven pathway in stallion sperm, as reported for other species.

Most notably, addition of 8pCPT induced rates of acrosomal exocytosis in capacitated stallion (34%) and mouse sperm (45%) comparable to those obtained with progesterone and/or calcium ionophore-treated sperm ($P > 0.05$). Because studies in somatic cells report effects of RAPGEF3/RAPGEF4 activation on specific membrane ion channels [31, 43–45] and RAPGEF3 localized to the acrosome in this study, we hypothesized a potential link between RAPGEF3 activation, changes in membrane potential, and acrosomal exocytosis.

It has been shown that capacitation-dependent hyperpolarization of the sperm plasma membrane is required for fertility [38]. In the mouse, this represents a change in membrane potential (E_m) from approximately −30 mV to approximately −60 mV, is dependent on the activation of various ion channels, and prepares the sperm for acrosomal exocytosis [39, 42, 46]. We report herein the resting membrane potential of

stallion sperm to be −37.11 mV and show that capacitated stallion sperm hyperpolarize to −53.74 mV ($P = 0.002$). In the mouse this hyperpolarization of the plasma membrane is postulated to occur via cAMP-PRKACA-mediated activation [41] followed by phosphorylation of the cystic fibrosis transmembrane conductor (CFTR). In turn, CFTR activation allows the influx of negatively charged Cl^- ions as well as the inhibition of the constitutively active epithelial sodium channels (ENaC), thus preventing the influx of Na^+ [39, 40]. Additionally, capacitation-associated increases in intracellular pH activate K^+_{ATP} channels, also contributing to membrane hyperpolarization [45].

Though RAPGEF3/RAPGEF4 activation with 8pCPT will induce hyperpolarization in cerebellar neurons [43], in various other excitable and nonexcitable somatic cells, RAPGEF3/RAPGEF4 activation has been observed to have effects on the abovementioned ion channels such that a depolarization of the plasma membrane would be expected. For instance, in pancreatic beta cells, Kang et al. [31, 44] observed a RAPGEF3/RAPGEF4-mediated inhibition of K^+_{ATP} channels; in rat pulmonary epithelial cells, 8pCPT increased the channel open probability of ENaC [47]; and, in rat hepatocytes, 8pCPT stimulated an outwardly rectifying Cl^- current [48]. In accordance, we demonstrate herein that incubation of stallion sperm under capacitating conditions in the presence of the RAPGEF3/RAPGEF4-selective agonist 8pCPT maintained stallion sperm E_m in the depolarized state, thus precluding membrane hyperpolarization as observed under the capacitating conditions.

Interestingly, previous work suggests that zona pellucida (ZP3)-induced acrosomal exocytosis results from plasma membrane depolarization [42, 46]. In this model, capacitation-dependent hyperpolarization results in the recruitment of low voltage-activated (LVA) T-type ion channels, which are then available for activation. Contact with ZP3 stimulates membrane depolarization and opening of LVA channels, thus resulting in calcium influx and the initiation of acrosomal exocytosis [42]. In our study, 1) RAPGEF3 localized to the acrosomal region of stallion and mouse sperm, 2) 8pCPT induced acrosomal exocytosis in capacitated stallion and mouse sperm, 3) 8pCPT did not induce acrosomal exocytosis in noncapacitated stallion sperm, and 4) 8pCPT maintained the stallion sperm membrane in the depolarized state. Based on these observations, we hypothesize that ZP3-directed RAPGEF3 activation is involved in the acrosome reaction-associated membrane depolarization possibly through its effects upon yet undetermined ion channels. This, in turn, may lead to the activation of LVA channels previously recruited as a result of capacitation-dependent hyperpolarization, followed by a sudden calcium influx and acrosomal exocytosis. Previous studies have demonstrated the presence of ENaC-δ in the acrosomal region of mouse sperm [38], colocalizing this ion channel with RAPGEF3. Additionally, ENaC-α localized to the midpiece of mouse sperm [38] and CFTR to the midpiece of both human and mouse sperm [41], colocalizing these ion channels with RAPGEF4. We therefore speculate that these ion channels could contribute to RAPGEF3-mediated changes in E_m and acrosomal exocytosis; future studies should aim at identifying the particular ion channels through which RAPGEF3 and/or RAPGEF4 may facilitate sperm membrane depolarization. Moreover, a voltage-gated proton channel (Hv1), an H^+ extrusion channel, has been recently identified as a major player in the alkalinization of CatSper channels and the subsequent Ca^{2+} influx required for sperm hyperactivation. Interestingly, this Hv1 channel is activated by membrane depolarization. Therefore, we cannot disregard the possibility that this and other ion channels may be identified as playing a role in our hypothesized pathway in future research [49].

Altogether, the results of this study present a novel role for cAMP-activated RAPGEF3/RAPGEF4 in mammalian sperm physiology, as it pertains to a role in acrosomal exocytosis and its effects on membrane potential. These results highlight the importance of contrasting the effects of RAPGEF3/RAPGEF4 and PRKACA, as both are cAMP-dependent proteins potentially playing specific and diverging roles in the events that lead to the acquisition of fertilization competency. Moreover, the dichotomy of different pathways (PRKACA vs. RAPGEF3/RAPGEF4) stemming from a common activator (cAMP) directing two different events—capacitation vs. acrosomal exocytosis—emphasizes the notion that sperm are highly specialized and compartmentalized cells. Future studies should be directed toward investigating the channels affected by RAPGEF3/RAPGEF4 activation and the resulting sperm membrane depolarization.

ACKNOWLEDGMENTS

The authors thank Ms. Carol Collyer and Drs. Katherine Beltaire, Valeria Tanco, Leticia Vivani, and Carlos Gradil for their assistance with semen collection from stallions. We also thank Dr. Eva Wertheimer for her assistance with membrane potential experiments and tracings (Fig. 9).

REFERENCES

1. Yanagimachi R. Mammalian Fertilization. In: Knobil E, Neill JD (eds.), The Physiology of Reproduction. New York, NY: Raven Press; 1994:189–317.
2. Galantino-Homer HL, Visconti PE, Kopf GS. Regulation of protein tyrosine phosphorylation during bovine sperm capacitation by a cyclic adenosine 3′5′-monophosphate-dependent pathway. Biol Reprod 1997; 56:707–719.
3. Visconti PE, Stewart-Savage J, Blasco A, Battaglia L, Miranda P, Kopf GS, Tezon JG. Roles of bicarbonate, cAMP, and protein tyrosine phosphorylation on capacitation and the spontaneous acrosome reaction of hamster sperm. Biol Reprod 1999; 61:76–84.
4. Osheroff JE, Visconti PE, Valenzuela JP, Travis AJ, Alvarez J, Kopf GS. Regulation of human sperm capacitation by a cholesterol efflux-stimulated signal transduction pathway leading to protein kinase A-mediated up-regulation of protein tyrosine phosphorylation. Mol Hum Reprod 1999; 5:1017–1026.
5. Visconti PE, Galantino-Homer H, Ning X, Moore GD, Valenzuela JP, Jorgez CJ, Alvarez JG, Kopf GS. Cholesterol efflux-mediated signal transduction in mammalian sperm. Beta-cyclodextrins initiate transmembrane signaling leading to an increase in protein tyrosine phosphorylation and capacitation. J Biol Chem 1999; 274:3235–3242.
6. Visconti PE, Westbrook VA, Chertihin O, Demarco I, Sleight S, Diekman AB. Novel signaling pathways involved in sperm acquisition of fertilizing capacity. J Reprod Immunol 2002; 53:133–150.
7. Suarez SS. Control of hyperactivation in sperm. Hum Reprod Update 2008; 14:647–657.
8. Pommer AC, Rutllant J, Meyers SA. Phosphorylation of protein tyrosine residues in fresh and cryopreserved stallion spermatozoa under capacitating conditions. Biol Reprod 2003; 68:1208–1214.
9. Ellington JE, Ball BA, Blue BJ, Wilker CE. Capacitation-like membrane changes and prolonged viability in vitro of equine spermatozoa cultured with uterine tube epithelial cells. Am J Vet Res 1993; 54:1505–1510.
10. Rathi R, Colenbrander B, Stout TA, Bevers MM, Gadella BM. Progesterone induces acrosome reaction in stallion spermatozoa via a protein tyrosine kinase dependent pathway. Mol Reprod Dev 2003; 64:120–128.
11. Christensen P, Whitfield CH, Parkinson TJ. In vitro induction of acrosome reactions in stallion spermatozoa by heparin and A23187. Theriogenology 1996; 45:1201–1210.
12. Meyers S, Kiu I, Overstreet J, Drobins E. Induction of acrosome reactions in stallion sperm by equine zona pellucida, porcine zona pellucida, and progesterone. Biol Reprod Mono 1995; 1:739–744.
13. Varner DD, Ward CR, Storey BT, Kenney RM. Induction and characterization of acrosome reaction in equine spermatozoa. Am J Vet Res 1987; 48:1383–1389.
14. Hinrichs K, Love CC, Brinsko SP, Choi YH, Varner DD. In vitro

fertilization of in vitro-matured equine oocytes: effect of maturation medium, duration of maturation, and sperm calcium ionophore treatment, and comparison with rates of fertilization in vivo after oviductal transfer. Biol Reprod 2002; 67:256–262.
15. Zhang JJ, Muzs LZ, Boyle MS. In vitro fertilization of horse follicular oocytes matured in vitro. Mol Reprod Dev 1990; 26:361–365.
16. Dell'Aquila ME, Fusco S, Lacalandra GM, Maritato F. In vitro maturation and fertilization of equine oocytes recovered during the breeding season. Theriogenology 1996; 45:547–560.
17. Dell'Aquila ME, Cho YS, Minoia P, Traina V, Lacalandra GM, Maritato F. Effects of follicular fluid supplementation of in-vitro maturation medium on the fertilization and development of equine oocytes after in-vitro fertilization or intracytoplasmic sperm injection. Hum Reprod 1997; 12:2766–2772.
18. Dell'Aquila ME, Cho YS, Minoia P, Traina V, Fusco S, Lacalandra GM, Maritato F. Intracytoplasmic sperm injection (ICSI) versus conventional IVF on abattoir-derived and in vitro-matured equine oocytes. Theriogenology 1997; 47:1139–1156.
19. Choi YH, Okada Y, Hochi S, Braun J, Sato K, Oguri N. In vitro fertilization rate of horse oocytes with partially removed zonae. Theriogenology 1994; 42:795–802.
20. Alm H, Torner H, Blottner S, Nurnberg G, Kanitz W. Effect of sperm cryopreservation and treatment with calcium ionophore or heparin on in vitro fertilization of horse oocytes. Theriogenology 2001; 56:817–829.
21. McPartlin LA, Littell J, Mark E, Nelson JL, Travis AJ, Bedford-Guaus SJ. A defined medium supports changes consistent with capacitation in stallion sperm, as evidenced by increases in protein tyrosine phosphorylation and high rates of acrosomal exocytosis. Theriogenology 2008; 69:639–650.
22. Visconti PE, Kopf GS. Regulation of protein phosphorylation during sperm capacitation. Biol Reprod 1998; 59:1–6.
23. Visconti PE, Moore GD, Bailey JL, Leclerc P, Connors SA, Pan D, Olds-Clarke P, Kopf GS. Capacitation of mouse spermatozoa, II: protein tyrosine phosphorylation and capacitation are regulated by a cAMP-dependent pathway. Development 1995; 121:1139–1150.
24. Hess KC, Jones BH, Marquez B, Chen Y, Ord TS, Kamenetsky M, Miyamoto C, Zippin JH, Kopf GS, Suarez SS, Levin LR, Williams CJ, et al. The ''soluble'' adenylyl cyclase in sperm mediates multiple signaling events required for fertilization. Dev Cell 2005; 9:249–259.
25. Holz GG, Kang G, Harbeck M, Roe MW, Chepurny OG. Cell physiology of cAMP sensor Epac. J Physiol 2006; 577:5–15.
26. Amano R, Lee J, Goto N, Harayama H. Evidence for existence of cAMP-Epac signaling in the heads of mouse epididymal spermatozoa. J Reprod Dev 2007; 53:127–133.
27. Branham MT, Mayorga LS, Tomes CN. Calcium-induced acrosomal exocytosis requires cAMP acting through a protein kinase A-independent, Epac-mediated pathway. J Biol Chem 2006; 281:8656–8666.
28. Aivatiadou E, Ripolone M, Brunetti F, Berruti G. cAMP-Epac2-mediated activation of Rap1 in developing male germ cells: RA-RhoGAP as a possible direct down-stream effector. Mol Reprod Dev 2009; 76:407–416.
29. Walsh DA, Ashby CD, Gonzalez C, Calkins D, Fischer EH, Krebs EG. Purification and characterization of a protein inhibitor of adenosine 3′,5′-monophosphate-dependent protein kinases. J Biol Chem 1971; 246:1977–1985.
30. Smolenski A, Bachmann C, Reinhard K, Honig-Leidi P, Jarchau T, Hoschuetzky H, Walter U. Analysis and regulation of vasodilator-stimulated phosphoprotein serine 239 phosphorylation in vitro and in intact cells using a phosphospecific monoclonal antibody. J Biol Chem 1998; 273:20029–20035.
31. Kang G, Chepurny OG, Malester B, Rindler MJ, Rehmann H, Bos JL, Schwede F, Coetzee WA, Holz GG. cAMP sensor Epac as a determinant of ATP-sensitive potassium channel activity in human pancreatic beta cells and rat INS-1 cells. J Physiol 2006; 573:595–609.
32. Travis AJ, Jorgez CJ, Merdiushev T, Jones BH, Dess DM, Diaz-Cueto L, Storey BT, Kopf GS, Moss SB. Functional relationships between capacitation-dependent cell signaling and compartmentalized metabolic pathways in murine spermatozoa. J Biol Chem 2001; 276:7630–7636.
33. Holmquist L. Surface modification of Beckman Ultra-Clear centrifuge tubes for density gradient centrifugation of lipoproteins. J Lipid Res 1982; 23:1249–1250.
34. Laemmli UK. Cleavage of structural proteins during the assembly of the head of bacteriophage T4. Nature 1970; 227:680–685.
35. Arcelay E, Saliconi, AM, Wertheimer EV, Visconti PE. Identification of proteins undergoing tyrosine phosphorylation during mouse sperm capacitation. Int J Dev Biol 2008; 52:462–472.
36. Selvaraj V, Buttke DE, Asano A, McElwee JL, Wolff CA, Nelson JL, Klaus AV, Hunnicutt GR, Travis AJ. GM1 dynamics as a marker for membrane changes associated with the process of capacitation in murine and bovine spermatozoa. J Androl 2007; 28:588–599.
37. Jungnickel MK, Marrero H, Birnbaumer L, Lemos JR, Florman HM. Trp2 regulates entry of Ca2+ into mouse sperm triggered by egg ZP3. Nat Cell Biol 2001; 3:499–502.
38. Demarco IA, Espinosa F, Edwards J, Sosnik J, De La Vega-Beltran JL, Hockensmith JW, Kopf GS, Darszon A, Visconti PE. Involvement of a Na+/HCO-3 cotransporter in mouse sperm capacitation. J Biol Chem 2003; 278:7001–7009.
39. Hernandez-Gonzalez EO, Sosnik J, Edwards J, Acevedo JJ, Mendoza-Lujambio I, Lopez-Gonzalez I, Demarco I, Wertheimer E, Darszon A, Visconti PE. Sodium and epithelial sodium channels participate in the regulation of the capacitation-associated hyperpolarization in mouse sperm. J Biol Chem 2006; 281:5623–5633.
40. Seino S, Shibasaki T. PKA-dependent and PKA-independent pathways for cAMP-regulated exocytosis. Physiol Rev 2005; 85:1303–1342.
41. Hernandez-Gonzalez EO, Trevino CL, Castellano LE, de la Vega-Beltran JL, Ocampo AY, Wertheimer E, Visconti PE, Darszon A. Involvement of cystic fibrosis transmembrane conductance regulator in mouse sperm capacitation. J Biol Chem 2007; 282:24397–24406.
42. Arnoult C, Kazam IG, Visconti PE, Kopf GS, Villaz M, Florman HM. Control of the low voltage-activated calcium channel of mouse sperm by egg ZP3 and by membrane hyperpolarization during capacitation. Proc Natl Acad Sci USA 1999; 96:6757–6762.
43. Ster J, De Bock F, Guerineau NC, Janossy A, Barrere-Lemaire S, Bos JL, Bockaert J, Fagni L. Exchange protein activated by cAMP (Epac) mediates cAMP activation of p38 MAPK and modulation of Ca2+-dependent K+ channels in cerebellar neurons. Proc Natl Acad Sci U S A 2007; 104:2519–2524.
44. Kang G, Leech CA, Chepurny OG, Coetzee WA, Holtz GG. Role of the cAMP sensor Epac as a determinant of KATP channel ATP sensitivity in human pancreatic beta-cells and rat INS-1 cells. J Physiol 2008; 586:1307–1319.
45. Muñoz-Garay C, De la Vega-Beltran JL, Delgado R, Labarca P, Felix R, Darszon A. Inwardly rectifying K(+) channels in spermatogenic cells: functional expression and implication in sperm capacitation. Dev Biol 2001; 234:261–274.
46. Florman HM, Jungnickel MK, Sutton KA. Regulating the acrosome reaction. Int J Dev Biol 2008; 52:503–510.
47. Helms MN, Chen XJ, Ramosevac S, Eaton DC, Jain L. Dopamine regulation of amiloride-sensitive sodium channels in lung cells. Am J Physiol Lung Cell Mol Physiol 2006; 290:L710–L722.
48. Aromataris EC, Roberts ML, Barritt GJ, Rychkov GY. Glucagon activates Ca2+ and Cl− channels in rat hepatocytes. J Physiol 2006; 573:611–625.
49. Lishko PV, Kirichok Y. The role of Hv1 and CatSper channels in sperm activation. J Physiol 2010; 588:4667–4672.